

Article

# Semi-Analytical Solution of Transverse Vibration of Cylinders with Non-Circular Cross-Section Partially Submerged in Water

Huixuan Han <sup>1,2</sup> , Yishuo Guo <sup>1</sup> and Ruili Huo <sup>3,\*</sup> 

<sup>1</sup> School of Civil Engineering and Architecture, Jiangsu University of Science and Technology, Zhenjiang 212100, China; huixuanhan@just.edu.cn (H.H.); yishuoguo01@126.com (Y.G.)

<sup>2</sup> School of Civil Engineering, Southeast University, Nanjing 210096, China

<sup>3</sup> College of Civil Engineering, Nanjing Tech University, Nanjing 211816, China

\* Correspondence: ruilihuo@njtech.edu.cn

**Abstract:** The free transverse vibration of a surface-piercing, vertical cylinder partially submerged in water was studied. The cylinder had an arbitrary non-circular, but symmetric, cross-section in the vibration direction. The water was assumed to be an incompressible and inviscid fluid. The effect of the surface waves of water was neglected in the analysis. The exact solution of velocity potential of water was derived by the method of separation of variables. The unknown coefficients in the solution of the velocity potential were expressed in the form of integral equations, including the dynamic deformation of the beam. Then, the governing differential equation of bending vibration of the cylinder under the hydrodynamic pressure was obtained. The Galerkin method was used to obtain the eigenvalue equation by expanding the wet modes of the cylinder into a series of dry modes. The elliptical cylinders partially submerged in water were taken as the numerical example. The accuracy of the proposed method was evaluated by the convergence studies. As a consequent result, the non-dimensional added virtual mass incremental (NAVMI) factor solutions were compared to the present Galerkin solutions, which can be used as a benchmark test for more sophisticated numerical simulations of computational fluid dynamics.

**Keywords:** fluid-structure interaction; non-circular column; free vibration; Galerkin solution; semi-analytical method



**Citation:** Han, H.; Guo, Y.; Huo, R. Semi-Analytical Solution of Transverse Vibration of Cylinders with Non-Circular Cross-Section Partially Submerged in Water. *J. Mar. Sci. Eng.* **2023**, *11*, 872. <https://doi.org/10.3390/jmse11040872>

Academic Editor: María Isabel Lamas Galdo

Received: 22 March 2023

Revised: 17 April 2023

Accepted: 18 April 2023

Published: 20 April 2023



**Copyright:** © 2023 by the authors. Licensee MDPI, Basel, Switzerland. This article is an open access article distributed under the terms and conditions of the Creative Commons Attribution (CC BY) license (<https://creativecommons.org/licenses/by/4.0/>).

## 1. Introduction

It is well known that structures in water behave differently from ones in air. Therefore, to understand the natural frequencies and modes of fluid–structure systems is of great importance for the study of structural responses to various excitations, such as earthquake loads, wind loads, and incident waves [1–3].

Cantilever cylinders are commonly encountered in offshore structures, such as intake towers, bridge piers, and stands of offshore oil platforms. Various methods have been applied to solve the problem of fluid–structure interactions, such as analytical methods [4,5], semi-analytical methods [6–9], and numerical methods [10–12].

It is generally accepted that numerical methods, such as finite element and boundary element methods, can deal with the fluid–structure interaction. Yang et al. [13] investigated the fundamental natural frequency of the free vibration of a rectangular cantilever beam partially immersed in water by using the finite element method and the experimental measure, respectively. Wang et al. [14] developed a finite element model to calculate the earthquake-induced hydrodynamic forces of cylinders with an arbitrary cross-section surrounded by water. Wei et al. [15] developed the simplified procedure for seismic design and the analysis of water-surrounded composite axisymmetric structures, and they proposed two types of formulations from analytical expression and finite element analysis, respectively. Zhang et al. [16] developed a three-dimensional finite element

model to evaluate the hydrodynamic added mass for cylinders with arbitrary cross-sections immersed in water. Liu [17] developed a frequency-domain software for wave–structure interactions based on the extended boundary integral equation method. However, it is well known that the modeling, code preparing, and numerically calculating adopted numerical methods require a long time. It may be especially difficult to properly handle the infinite boundary of water and conduct a parametric analysis.

Han and Xu [18] derived the analytical expressions of natural frequencies and mode shapes for a completely immersed cantilever cylinder with a circular cross-section and proposed a simple formula to evaluate the natural frequencies by using the added mass conception. Wang et al. [19] presented a simple added mass model for the dynamic analysis of a flexible elliptical cylinder entirely submerged in deep water based on the analytical solution for the hydrodynamic forces. Their solution was complex due to the requirement of dealing with the infinite series of the Mathieu functions in the elliptical cylindrical coordinates. The analytical method was also applied by Yu et al. [20] to obtain the distribution of the added water mass for a cantilever cylinder partially submerged in water. On this basis, they proposed a simplified calculation method to investigate the fundamental natural frequency of a circular cross-sectional immersed cylinder, which is in good agreement with their experimental results. The analytical methods can provide the exact solutions; however, they are only limited to very special and simple cases. Semi-analytical methods, which combine the advantages of the wide applicability of numerical methods and the high accuracy of analytical methods, can solve the problem at a small computational cost.

The early study on hydrodynamics can trace back to the motion of rigid bodies in fluid, as discussed in references [12,21], by considering that the effect of the fluid on the motion of the body is equivalent to an added virtual mass, which represents a force induced in the fluid domain proportional to the acceleration of the fluid. Since then, the study was further expanded to wave forces on the rigid bodies, as described by Williams [22]. Investigations revealed that, in many cases, the rigid assumption of the structures is not applicable, and the flexibility of structures has considerable influence on the dynamic behavior of the fluid–structure system [18,19,23,24]. Lin et al. [8], McCormick [25], Williams [26], and Han and Xu [18] investigated the vibratory characteristics of uniform cylinders partially submerged in water, and the concept of added virtual mass was extended to include the effect of vibration modes. In recent years, the simplified formulas for calculating the added hydrodynamic mass of elliptical, round-ended, hollow, and rectangular cylinders, as well as axisymmetric structures, were developed by Wang et al. [14,19], Yang and Li [27], Zhao et al. [28], and Wei et al. [15], respectively. However, up until now, most of the studies focused on cylinders with circular cross-sections, such as the references [5,18,20,24–26]. Except for several papers using elliptical cross-sections [19,22,29], few cylinders with non-circular cross-sections [6,9] have been studied. In fact, the analytical methods mentioned above are not able to deal with the cylinders with general cross-sections (such as rectangle and triangle). Additionally, the accuracy of the added virtual mass approach has not been evaluated properly, although the concept of the added virtual mass has been commonly used in the approximate analysis of fluid–structure interaction.

The purpose of this paper was to develop a general semi-analytical method for studying the hydroelastic behavior of uniform slender cylinders partially submerged in water with arbitrary non-circular cross-sections. Based on the orthogonality and completeness of trigonometric series, the velocity potential function of water was expanded into a Fourier series along the external surface of the cylinder. The exact solution of motion of the water was derived by using the method of separation of variables in the cylinder coordinate system. The Galerkin method was applied to obtain the eigenfrequency equation of the cylinder under the hydrodynamic pressure. The results for elliptical cylinders partially submerged in water, taken as the numerical example, were studied in detail. It was shown that this method has high accuracy and small computational cost. The analysis process is relatively simple and suitable for arbitrary non-circular cross-sections, which involves no particularly complex mathematical equations, such as Mathieu functions for elliptical

cross-sections. The accuracy of the commonly used NAVMI (non-dimensional added virtual mass incremental) factor solutions in engineering was evaluated by comparing them to the present Galerkin solutions. The results of this study provide a benchmark test for simulating more complex fluid–structure interactions.

## 2. Semi-Analytical Method

### 2.1. Governing Equations of Fluid–Structure Interaction

Consider a uniform slender solid or hollow cylinder with an arbitrary non-circular cross-section, as shown in Figure 1. The surface-piercing cylinder is surrounded by infinite water of depth  $h$  and makes transverse free vibration in the  $x$  direction. The cylinder, which is treated as a one-dimensional elastic beam, has a length  $H$  and a symmetric cross-section  $F$  about the  $x$  axis. The mass of the cylinder per unit length is  $\rho_0 F$ , and the flexural stiffness of the cylinder is  $EI$ . Assuming that the cylinder is acted upon by a transversely distributed liquid pressure  $P(z, t)$  along its axis in the interval  $(0, h)$  ( $h \leq H$ ), then the governing differential equation of motion of the elastic cylinder can be described by the Bernoulli-Euler beam theory, as follows:

$$EI \frac{\partial^4 y}{\partial z^4} + \rho_0 F \frac{\partial^2 y}{\partial t^2} = \begin{cases} 0 & h \leq z \leq H \\ P(z, t) & 0 \leq z < h \end{cases} \quad (1)$$

where  $y(z, t)$  is the dynamic deformation of the cylinder, and  $t$  is time. The bending moment  $M(z, t)$  and shear force  $V(z, t)$  of the cylinder are shown, respectively, as follows:

$$M(z, t) = EI \frac{\partial^2 y}{\partial z^2}, \quad V(z, t) = -EI \frac{\partial^3 y}{\partial z^3} \quad (2)$$

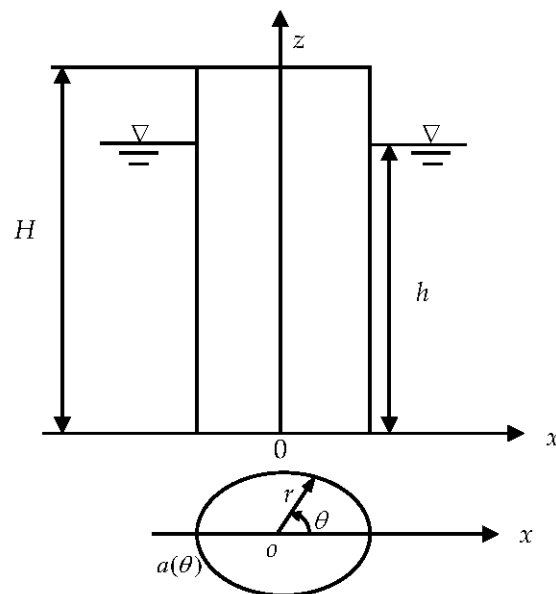


Figure 1. The cylinder with a non-circular cross-section partially submerged in water.

Since cantilever cylinders are common in offshore structures, a cylinder fixed at the bottom and free at the top was taken as an example without loss of generality. Thus, the boundary conditions of the cantilever beam are shown, respectively, as follows:

$$y = 0, \quad \frac{\partial y}{\partial z} = 0, \quad \text{at } z = 0 \quad (3)$$

$$\frac{\partial^2 y}{\partial z^2} = 0, \quad \frac{\partial^3 y}{\partial z^3} = 0, \quad \text{at } z = H \quad (4)$$

In order to analyze the motion of the water surrounding the cylinder, cylindrical coordinates  $(o, r, \theta, z)$  are established, as shown in Figure 1. The water is treated as an ideal, incompressible, and inviscid fluid. It is further assumed that the wave heights of the water are sufficiently small, such that its effect on the vibration of the cylinder can be neglected. Subjected to the above restrictions and assumptions, the motion of the water may be described in terms of a velocity potential  $\phi(r, \theta, z, t)$  satisfying the Laplace equation in the flow region as follows:

$$\frac{\partial^2 \phi}{\partial r^2} + \frac{1}{r} \frac{\partial \phi}{\partial r} + \frac{1}{r^2} \frac{\partial^2 \phi}{\partial \theta^2} + \frac{\partial^2 \phi}{\partial z^2} = 0 \tag{5}$$

The relations between the velocity potential and the velocities of water are:

$$v_r = \frac{\partial \phi}{\partial r}, v_\theta = \frac{1}{r} \frac{\partial \phi}{\partial \theta}, v_z = \frac{\partial \phi}{\partial z} \tag{6}$$

The boundary conditions to  $\phi(r, \theta, z, t)$  are:

$$\frac{\partial \phi}{\partial z} = 0, \text{ at } z = 0, \frac{\partial \phi}{\partial t} = 0, \text{ at } z = h, \frac{\partial \phi}{\partial t} = 0, r \rightarrow \infty \tag{7}$$

$$\nabla \phi \bullet \vec{n} = \frac{\partial y}{\partial t} (\vec{n} \bullet \vec{x}), \text{ at } r = a_0 a(\theta) \tag{8}$$

where  $\nabla$  is the gradient operator,  $\vec{n}$  is the outward unit normal vector of the cylinder surface,  $\vec{x}$  is the unit vector in the  $x$  direction, and  $\vec{\theta}$  is that in the  $\theta$  direction.  $r = a_0 a(\theta)$  is the equation of the external surface of the cylinder, where  $a_0$  is the characteristic size of the cross-section (in most cases,  $a_0$  takes the maximum radial size of the cross-section).

### 2.2. Solution of Velocity Potential

Consider that the cylinder makes free vibration. Both  $y(z, t)$  and  $\phi(r, \theta, z, t)$  are the harmonic functions of time and have the same vibratory frequency  $\omega$  (natural radian frequency of the cylinder–water system). Then, the dynamic deformation of the cylinder  $y(z, t)$  and the velocity potential  $\phi(r, \theta, z, t)$  can be assumed in the form of separated variables, respectively, as follows: The method of separating variables is as follows

$$y(z, t) = Y(z)e^{-i\omega t}, \phi(r, \theta, z, t) = R(r)\Theta(\theta)Z(z)e^{-i\omega t} \tag{9}$$

By substituting Equation (9) into Equation (5), three ordinary differential equations can be obtained by separating variables [30] (pp. 183–185). Then, solving these equations and combining the boundary conditions in Equation (7) gives the following:

$$\phi(r, \theta, z, t) = -i\omega e^{-i\omega t} \left\{ \sum_{n=0}^{\infty} \sum_{j=0}^{\infty} C_n^j K_n(\alpha_j \frac{\beta}{\mu} \chi) \cos(\frac{\alpha_j}{\mu} \zeta) \cos(n\theta) + \sum_{n=1}^{\infty} \sum_{j=0}^{\infty} \bar{C}_n^j K_n(\alpha_j \frac{\beta}{\mu} \chi) \cos(\frac{\alpha_j}{\mu} \zeta) \sin(n\theta) \right\} \tag{10}$$

where  $C_n^j$  and  $\bar{C}_n^j$  are the unknown constants, and  $K_n$  is the modified Bessel functions of the second kind of order  $n$ . In Equation (10), the following non-dimensional parameters and coordinates are introduced:

$$\alpha_j = (j + 0.5)\pi, \beta = a_0/H, \mu = h/H, \chi = r/a_0, \zeta = z/H \tag{11}$$

in which,  $\beta$  is the aspect ratio of the cylinder and  $\mu$  cylinder-water size factor.

By substituting Equation (10) into Equation (8) and considering the symmetry of the cross-section of the cylinder about the  $x$  axis, the following is obtained:

$$\bar{C}_n^j = 0, n = 1, 2, 3, \dots, j = 0, 1, 2, \dots \tag{12}$$

$$\sum_{n=0}^{\infty} \sum_{j=0}^{\infty} C_n^j g_n^j(\theta) N(\theta) \cos\left(\frac{\alpha_j}{\mu} \zeta\right) = a_0 e(\theta) N(\theta) Y(\zeta), 0 \leq \zeta \leq \mu \tag{13}$$

where

$$g_n^j(\theta) = \alpha_j \frac{\beta}{\mu} a(\theta) \dot{K}_n\left(\alpha_j \frac{\beta}{\mu} a(\theta)\right) \cos(n\theta) + n \frac{\dot{a}(\theta)}{a(\theta)} K_n\left(\alpha_j \frac{\beta}{\mu} a(\theta)\right) \sin(n\theta) \tag{14}$$

$$N(\theta) = 1/\sqrt{a(\theta)^2 + \dot{a}(\theta)^2}, e(\theta) = a(\theta) \cos(\theta) + \dot{a}(\theta) \sin(\theta) \tag{15}$$

in which,  $\dot{K}_n(r) = dK_n(r)/dr$  and  $\dot{a}(\theta) = da(\theta)/d\theta$ .

Considering the orthogonality among cosine functions  $\cos(\frac{\alpha_j}{\mu} \zeta)$  ( $j = 1, 2, 3, \dots$ ) in the interval  $[0, \mu]$ , that is:

$$\int_0^{\mu} \cos\left(\frac{\alpha_j}{\mu} \zeta\right) \cos\left(\frac{\alpha_i}{\mu} \zeta\right) d\zeta = \frac{\mu}{2} \delta(i - j) \tag{16}$$

Multiplying  $\cos(\frac{\alpha_j}{\mu} \zeta)$  to two sides of Equation (13), then making the integration about  $\zeta$  in the interval  $[0, \mu]$ , one can obtain the following:

$$\sum_{n=0}^{\infty} C_n^j g_n^j(\theta) N(\theta) = \frac{2a_0}{\mu} e(\theta) N(\theta) \int_0^{\mu} Y(\zeta) \cos\left(\frac{\alpha_j}{\mu} \zeta\right) d\zeta, j = 0, 1, 2, \dots \tag{17}$$

Further, by making the Fourier expansion to the above equation for the circumferential coordinate  $\theta$  in the interval  $[0, \pi]$ , the following can be obtained:

$$\begin{bmatrix} S_{00}^j & S_{01}^j & \dots & S_{0N}^j \\ S_{10}^j & S_{11}^j & \dots & S_{1N}^j \\ \vdots & \vdots & \ddots & \vdots \\ S_{N0}^j & S_{N1}^j & \dots & S_{NN}^j \end{bmatrix} \begin{bmatrix} C_0^j \\ C_1^j \\ \vdots \\ C_N^j \end{bmatrix} = 2 \frac{a_0}{\mu} G_j \begin{bmatrix} Q_0 \\ Q_1 \\ \vdots \\ Q_N \end{bmatrix}, j = 0, 1, 2, \dots \tag{18}$$

where  $N$  is the order of the Fourier expansion and

$$S_{in}^j = \int_0^{\pi} g_n^j(\theta) N(\theta) \cos(i\theta) d\theta, Q_i = \int_0^{\pi} e(\theta) N(\theta) \cos(i\theta) d\theta \tag{19}$$

$$G_j = \int_0^{\mu} Y(\zeta) \cos\left(\frac{\alpha_j}{\mu} \zeta\right) d\zeta \tag{20}$$

Introducing the following formula to Equation (18):

$$\begin{bmatrix} D_0^j \\ D_1^j \\ \vdots \\ D_N^j \end{bmatrix} = \begin{bmatrix} S_{00}^j & S_{01}^j & \dots & S_{0N}^j \\ S_{10}^j & S_{11}^j & \dots & S_{1N}^j \\ \vdots & \vdots & \ddots & \vdots \\ S_{N0}^j & S_{N1}^j & \dots & S_{NN}^j \end{bmatrix}^{-1} \begin{bmatrix} Q_0 \\ Q_1 \\ \vdots \\ Q_N \end{bmatrix} \tag{21}$$

one has:

$$C_n^j = 2 \frac{a_0}{\mu} G_j D_n^j, n = 0, 1, 2, \dots, N, j = 0, 1, 2, \dots, J \tag{22}$$

Finally, the exact solution of the velocity potential of the water can be given by:

$$\phi(\chi, \theta, \zeta, t) = -2\omega \frac{a_0}{\mu} i e^{-i\omega t} \sum_{n=0}^N \sum_{j=0}^J D_n^j G_j K_n(\alpha_j \frac{\beta}{\mu} \chi) \cos(\frac{\alpha_j}{\mu} \zeta) \cos(n\theta) \tag{23}$$

In the above equation, the integral equations  $G_j$  ( $j = 0, 1, 2, \dots, J$ ), which represent the coupling effect of the cylinder and the water, are dealt with later.

### 2.3. Eigenvalue Equation

From the Bernoulli equation in fluid mechanics, the dynamic pressure distribution  $p(\zeta, t)$  of water on the external surface of the cylinder is:

$$p(\zeta, t) = -\rho_1 \frac{\partial \phi}{\partial t} \Big|_{\chi=a(\theta)} \tag{24}$$

where  $\rho_1$  is the density of the water. Therefore, the resultant force  $P(\zeta, t)$  of the water dynamic pressure on the cylinder per unit length is:

$$P(\zeta, t) = -2a_0 \int_0^\pi p(\zeta, t) (\vec{n} \bullet \vec{x}) \sqrt{a(\theta)^2 + \dot{a}(\theta)^2} d\theta \tag{25}$$

Substituting Equations (23) and (24) into the above equation gives:

$$P(\zeta, t) = -4 \frac{a_0^2}{\mu} \rho_1 \omega^2 e^{-i\omega t} \sum_{n=0}^N \sum_{j=0}^J D_n^j G_j \cos(\frac{\alpha_j}{\mu} \zeta) I_n^j \tag{26a}$$

in which,

$$I_n^j = \int_0^\pi K_n(\alpha_j \frac{\beta}{\mu} a(\theta)) e(\theta) \cos(n\theta) d\theta \tag{26b}$$

By substituting Equations (26a) and (9) into Equation (1), one can obtain the following:

$$\frac{d^4 Y(\zeta)}{d\zeta^4} - \lambda^2 Y(\zeta) = \begin{cases} 0 & \mu \leq \zeta \leq 1 \\ -4 \frac{\gamma}{\mu} \lambda^2 \sum_{n=0}^N \sum_{j=0}^J D_n^j G_j I_n^j \cos(\frac{\alpha_j}{\mu} \zeta) & 0 \leq \zeta < \mu \end{cases} \tag{27}$$

where  $\lambda$  is the non-dimensional frequency parameter, and  $\gamma$  is the cylinder–water density factor, as follows:

$$\lambda^2 = \frac{\rho_0 F}{EI} \omega^2 H^4, \quad \gamma = \frac{\rho_1 a_0^2}{\rho_0 F} \tag{28}$$

In the following analysis, the Galerkin method is applied to derive the eigenvalue equation from Equation (28). Assuming that the wet mode  $Y(\zeta)$  of the cylinder can be expanded by the dry modes of the cylinder  $\tilde{Y}_l(\zeta)$  ( $l = 1, 2, 3, \dots$ ) in the form of:

$$Y(\zeta) = \sum_{l=1}^L A_l \tilde{Y}_l(\zeta) \tag{29}$$

where  $A_l$  ( $l = 1, 2, 3, \dots, L$ ) are the unknown constants,  $L$  is the truncated order of the dry modes. For a cantilever beam,  $\tilde{Y}_l(\zeta)$  are as follows:

$$\tilde{Y}_l(\zeta) = \cosh(k_l \zeta) - \cos(k_l \zeta) - \frac{\sinh k_l - \sin k_l}{\cosh k_l + \cos k_l} [\sinh(k_l \zeta) - \sin(k_l \zeta)] \tag{30}$$

in which,  $k_l$  satisfies:

$$\cosh(k_l) \cos(k_l) = 1, \quad l = 1, 2, 3, \dots, L \tag{31}$$

It is obvious that all of  $\tilde{Y}_l(\zeta)$  exactly satisfy the boundary conditions (3) and (4).

By substituting Equation (29) into Equation (28), then multiplying the two sides of Equation (28) by  $\tilde{Y}_i(\zeta)$  ( $i = 1, 2, 3, \dots, L$ ), and integrating the equation from 0 to 1, one can obtain the following eigenvalue equation:

$$\{[K] - \lambda^2([I] + \gamma[\tilde{M}])\}\{A\} = 0 \tag{32}$$

where

$$[K] = \begin{bmatrix} k_1^4 & & & \\ & k_2^4 & 0 & \\ & 0 & \ddots & \\ & & & k_L^4 \end{bmatrix}, [\tilde{M}] = \begin{bmatrix} \tilde{m}_{11} & \tilde{m}_{12} & \cdots & \tilde{m}_{1L} \\ \tilde{m}_{21} & \tilde{m}_{22} & \cdots & \tilde{m}_{2L} \\ \vdots & \vdots & \ddots & \vdots \\ \tilde{m}_{L1} & \tilde{m}_{L2} & \cdots & \tilde{m}_{LL} \end{bmatrix} \tag{33}$$

$$[I] = \begin{bmatrix} 1 & & & \\ & 1 & 0 & \\ & 0 & \ddots & \\ & & & 1 \end{bmatrix}, \{A\} = \begin{Bmatrix} A_1 \\ A_2 \\ \vdots \\ A_L \end{Bmatrix}$$

in which,

$$\tilde{m}_{il} = -\frac{4}{\mu} \sum_{n=0}^{\infty} \sum_{j=0}^{\infty} D_n^j q_j^i q_j^l, i, l = 1, 2, 3, \dots, L \tag{34}$$

$$q_j^i = \int_0^1 \tilde{Y}_i(k_i \zeta) \cos\left(\frac{\alpha_j}{\mu} \zeta\right) d\zeta \tag{35}$$

In Equation (33), the orthogonal relations among  $\tilde{Y}_l(k_l \zeta)$  ( $l = 1, 2, 3, \dots, L$ ) were used. Matrix  $[\tilde{M}]$  represents the effect of water on the dynamic characteristics of the cylinder and is called the non-dimensional added virtual mass incremental (NAVMI) matrix. The diagonal elements  $\tilde{m}_{ii}$  ( $i = 1, 2, \dots, L$ ) are called NAVMI factors, which are discussed in following analysis.

### 3. Convergence Studies

In order to verify the applicability of the method proposed, the convergence study was carried out for solid elliptical cylinders. The external surface equation of the elliptical cylinder is:

$$a(\theta) = (b_0/a_0) / \sqrt{(b_0/a_0)^2 \sin^2(\theta) + \cos^2(\theta)} \tag{36}$$

Two different cylinder–water size factors,  $\mu = h/H = 1.0; 0.8$ , and two different cross-sectional size factors,  $b_0/a_0 = 1.0; 0.5$ , were considered for the convergence study. In the computations, unless otherwise stated, the following parameters were used: water density  $\rho_1 = 1000 \text{ kg/m}^3$ ; cylinder density  $\rho_0 = 2450 \text{ kg/m}^3$ ; and aspect ratio of the cylinder  $\beta = a_0/H = 0.1$ .

The exact solution of the velocity potential of the water  $\phi(\chi, \theta, \zeta, t)$  in Equation (23) is numerically stable and converges rapidly with the increase of terms  $N$  and  $J$ . When  $N = 20$  and  $J = 40$ , it is sufficient to guarantee the accuracy of the solution  $\phi(\chi, \theta, \zeta, t)$  to five significant digits. Therefore, 20 terms about  $N$  and 40 terms about  $J$  were enough for the present analysis without losing accuracy.

In order to verify the convergence of the present method, Table 1 gives the first five non-dimensional frequency parameters  $\sqrt{\lambda_i}$  ( $i = 1, 2, 3, 4, 5$ ) of the cylinder–water interaction by using a different number  $L$  of vibrating beam functions, steadily increasing from 3 to 6. It can be observed that the results in Table 1 are convergent with the increase term of  $L$ , and the slight difference between  $L = 5$  and  $L = 6$  assures the accuracy and the rapid convergence rate. It is seen that the influence of the cross-sectional size factor of the cylinder  $b_0/a_0$  and the cylinder–water size factor  $\mu$  on the convergence rate is relatively small. However, it can be seen from Table 1 that the convergence rate of the elliptical cylinder ( $b_0/a_0 = 0.5$ ) is slightly slower than that of the circular cylinder ( $b_0/a_0 = 1.0$ ). The convergence rate of the fully submerged cylinder ( $\mu = 1.0$ ) is faster than that of the partially submerged cylinder

( $\mu = 0.8$ ). In Table 1, it is also seen that the natural frequencies of the cylinder in water are always smaller than those in air.

**Table 1.** The non-dimensional frequency parameters of elliptical cylinders partially submerged in water, using a different number of terms of vibrating beam functions ( $N = 20, J = 40$ ).

$b_0/a_0$	$\mu$	$L$	$\sqrt{\lambda_1}$	$\sqrt{\lambda_2}$	$\sqrt{\lambda_3}$	$\sqrt{\lambda_4}$	$\sqrt{\lambda_5}$
1.0	1.0	3	1.76214	4.40831	7.42111		
		4	1.76214	4.40830	7.42033	10.45594	
		5	1.76214	4.40830	7.42033	10.45483	13.51868
		6	1.76214	4.40830	7.42029	10.45483	13.51737
	0.8	3	1.82937	4.45475	7.47621		
		4	1.82937	4.45474	7.47374	10.55185	
		5	1.82937	4.45474	7.47367	10.54663	13.63776
		6	1.82937	4.45473	7.47360	10.54646	13.63005
0.5	1.0	3	1.66802	4.17647	7.04960		
		4	1.66802	4.17644	7.04755	9.96702	
		5	1.66802	4.17642	7.04752	9.96387	12.93266
		6	1.66802	4.17642	7.04740	9.96386	12.92871
	0.8	3	1.78331	4.27320	7.15348		
		4	1.78331	4.27316	7.14618	10.14705	
		5	1.78331	4.27315	7.14590	10.12947	13.17693
		6	1.78331	4.27315	7.14573	10.12872	13.15165
Dry modes			1.87510	4.69409	7.85476	10.99554	14.13717

In general, 6 terms about  $L$ , 20 terms about  $N$ , and 40 terms about  $J$  could provide the first five frequencies with sufficiently satisfactory accuracy; hence they are used in the following calculations.

#### 4. Results and Discussion

##### 4.1. NAVMI Factor Solutions

In engineering, the NAVMI factor approach is usually used for approximate analysis by considering the effect of water as the equivalent added virtual mass on vibration modes of structures. Observing Equation (32), one can find that if the NAVMI matrix  $[\tilde{M}]$  is diagonal (its non-diagonal elements are neglected), then the non-dimensional natural frequency  $\lambda$  can be obtained simply and directly from Equation (32); that is,  $\lambda_i = k_i^2 \sqrt{1 + \gamma \tilde{m}_{ii}}$  ( $i = 1, 2, 3, \dots, L$ ). This assumes that the wet modes of the cylinder in water are similar to the dry modes of the cylinder in air. At this point, a corresponding NAVMI factor  $\tilde{m}_{ii}$  is added to each dry mode of the cylinder, which means that the effect of water only modifies the mass of each dry mode. However, the actual NAVMI matrix  $[\tilde{M}]$  is not a diagonal one. Therefore, using the NAVMI factor approach that considers only diagonal elements of the NAVMI matrix  $[\tilde{M}]$  to estimate the natural frequency of the cylinder–water interaction may lead to a certain error, which should be carefully evaluated. Still, taking cylinders considered in the preceding section as an example and using five vibrating beam functions in the computation, one has:

$$[\tilde{M}] = \begin{bmatrix} 2.296042 & 0.54951 & -0.28841 & 0.26260 & -0.14763 \\ 0.54951 & 2.33897 & 0.41394 & -0.13511 & 0.24106 \\ -0.28841 & 0.41397 & 2.13281 & 0.31866 & -0.04891 \\ 0.26260 & -0.13511 & 0.31866 & 1.89388 & 0.25115 \\ -0.14763 & 0.24106 & -0.04891 & 0.25115 & 1.68177 \end{bmatrix} \quad (37)$$

for an elliptical cylinder ( $b_0/a_0 = 0.5$ ) with a cylinder–water size factor of  $\mu = 1.0$  and

$$[\tilde{M}] = \begin{bmatrix} 0.84962 & 1.04825 & -0.26678 & -0.05605 & 0.24164 \\ 1.04825 & 1.98485 & 0.61417 & -0.20547 & 0.20856 \\ -0.26678 & 0.61417 & 1.85430 & 0.58603 & -0.23336 \\ -0.05605 & -0.20547 & 0.58603 & 1.55282 & 0.54830 \\ 0.24164 & 0.20856 & -0.23336 & 0.54830 & 1.37745 \end{bmatrix} \quad (38)$$

for the elliptical cylinder with the cylinder–water size factor  $\mu = 0.8$ .

It is seen that, when the cylinder is entirely submerged in water ( $\mu = 1.0$ ), the NAVMI matrix has a dominance of diagonal elements over the others. In this case, the mode parameters can be accurately estimated by the NAVMI factor approach. However, when the cylinder is partially submerged in water ( $\mu = 0.8$ ), the matrix is not diagonally dominant. In this case, larger errors would occur if the mode parameters were derived using the NAVMI factor approach.

To evaluate the accuracy of the NAVMI factor approach, the NAVMI factor solutions obtained by simplifying the NAVMI matrix  $[\tilde{M}]$  to a diagonal one were compared with the solutions from the accurate non-diagonal one.  $\tilde{\lambda}$  and  $\lambda$  represent the non-dimensional natural frequency of the NAVMI factor solutions and the Galerkin solutions, respectively. Then, the error between the  $i$ th non-dimensional natural frequency of the NAVMI factor solutions with respect to that of the Galerkin solutions was defined by  $e_i = (1 - \tilde{\lambda}_i/\lambda_i)$ . Figures 2 and 3 give the percentage errors  $e_i$  ( $i = 1, 2, \dots, 6$ ) of the first six natural frequencies of the NAVMI factor solutions, with respect to those of the Galerkin solutions, respectively, for entirely ( $\mu = 1.0$ ) and partially ( $\mu = 0.8$ ) submerged elliptical cylinders ( $b_0/a_0 = 0.5$ ), as the function of the cylinder–water density factor  $\gamma$ . As can be seen in Figures 2 and 3, the simplification of the NAVMI matrix to a diagonal one results in different errors in different cases. It is seen that the errors of the NAVMI factor solutions for the partially submerged cylinder ( $\mu = 0.8$ ) are greatly larger than those for the entirely submerged cylinder ( $\mu = 1.0$ ). However, in all the cases, the errors for the fundamental frequency are always relatively small. The larger the cylinder–water density factor, the larger the errors of the frequencies are.

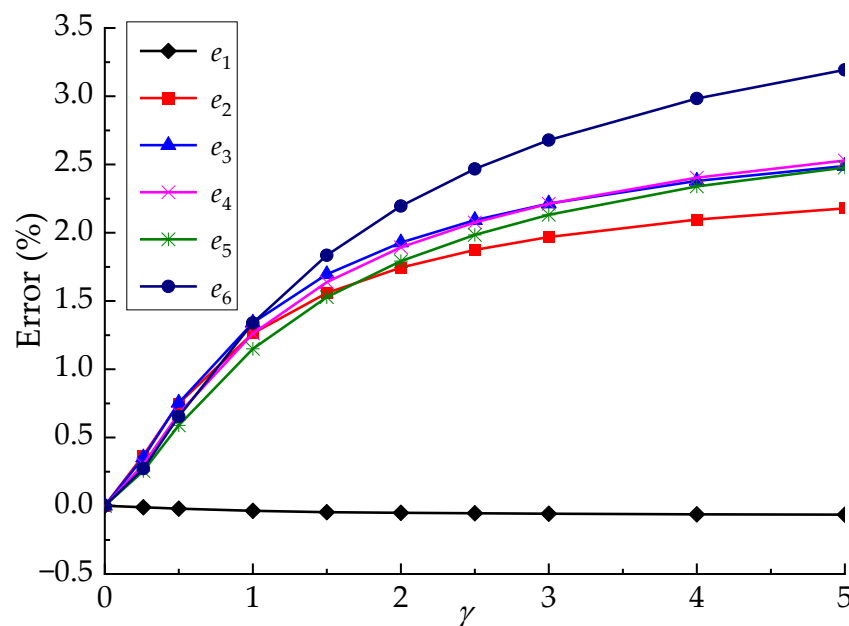


**Figure 2.** The percentage errors of the first six natural frequencies of the NAVMI factor solutions with respect to the Galerkin solutions for an entirely submerged ( $\mu = 1.0$ ) elliptical cylinder ( $b_0/a_0 = 0.5$ ), as the function of the cylinder–water density factor  $\gamma$ .

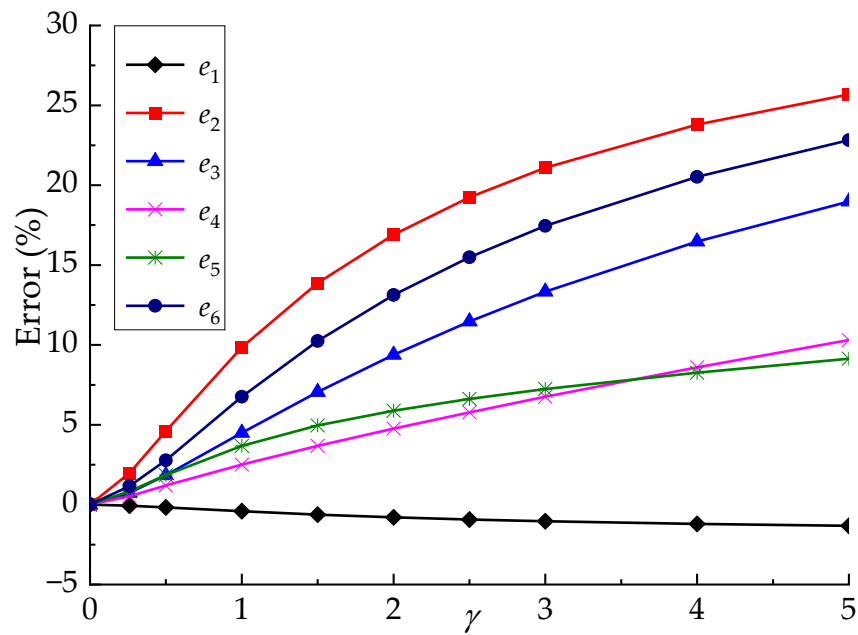


**Figure 3.** The percentage errors of the first six natural frequencies of the NAVMI factor solutions with respect to the Galerkin solutions for a partially submerged ( $\mu = 0.8$ ) elliptical cylinder ( $b_0/a_0 = 0.5$ ), as the function of the cylinder–water density factor  $\gamma$ .

The percentage errors of the first six natural frequencies of the NAVMI factor solutions with respect to the Galerkin solutions for partially submerged elliptical cylinders ( $b_0/a_0 = 0.5$ ), with the cylinder–water density factor  $\gamma = 5.0$  as the function of the cylinder–water size factor  $\mu$ , are given in Figure 4. It is shown in Figure 4 that the errors of natural frequencies between the NAVMI factor solutions and the Galerkin solutions vary with the cylinder–water size factor  $\mu$  by a big margin, except for fundamental frequency. It should be noted that the maximum errors of frequencies do not occur at  $\mu = 1.0$ ; however, they do among  $\mu = 0.3\sim 0.7$ .

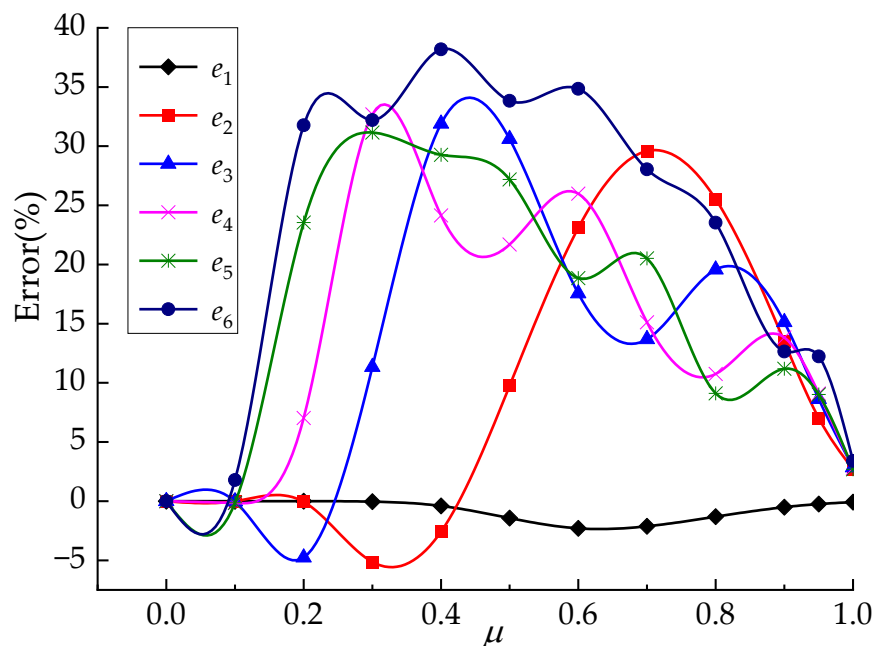


**Figure 4.** The percentage errors of the first six natural frequencies of the NAVMI factor solutions with respect to the Galerkin solutions for a partially submerged elliptical cylinder ( $b_0/a_0 = 0.5$ ) with a cylinder–water density factor of  $\gamma = 5.0$ , as a function of the cylinder–water size factor  $\mu$ .

From the above analysis, one can conclude that the fundamental frequency of the cylinder–water interaction can always be accurately estimated by the NAVMI factor approach. However, the frequencies more than the second order can be accurately estimated only for very small cylinder–water density factors  $\gamma$  and cylinder aspect ratios  $\beta$ , especially when the cylinder is partially submerged in water.

4.2. Numerical Results

In this section, the elliptical cylinders partially submerged in water are investigated numerically. The densities of the cylinder and water are the same as those used in Section 3. Six terms for  $L$ , twenty terms for  $N$ , and forty terms for  $J$  were taken in the following computations. Three different cross-sectional size factors  $b_0/a_0 = 0.5; 1.0; 2.0$ , two different aspect ratios  $\beta = 0.05; 0.1$ , and two different cylinder–water size factors  $\mu = 0.8; 1.0$  were considered. The first six non-dimensional frequency parameters  $\sqrt{\lambda_i}$  ( $i = 1, 2, \dots, 6$ ) are given in Table 2.

**Table 2.** The first six non-dimensional frequency parameters of elliptical cylinders submerged in water for different aspect ratios  $\beta$  of the cylinder and cylinder–water size factor  $\mu$ .

$\beta$	$\mu$	$\sqrt{\lambda_1}$	$\sqrt{\lambda_2}$	$\sqrt{\lambda_3}$	$\sqrt{\lambda_4}$	$\sqrt{\lambda_5}$	$\sqrt{\lambda_6}$
$b_0/a_0 = 0.5$							
0.05	0.8	1.76816	4.24859	7.04660	9.93900	12.89451	15.87104
	1.0	1.64492	4.11938	6.92178	9.74505	12.60615	15.50506
0.1	0.8	1.78330	4.27310	7.14564	10.12862	13.15153	16.18568
	1.0	1.66800	4.17636	7.04731	9.96374	12.92856	15.93466
$b_0/a_0 = 1.0$							
0.05	0.8	1.82007	4.43447	7.40232	10.42459	13.47035	16.51177
	1.0	1.74523	4.36876	7.33377	10.30927	13.31098	16.33582
	1.0	(1.77103) [1.74192]	(4.42978) —	(7.40222) —	— —	— —	— —
0.1	0.8	1.82937	4.45473	7.47360	10.54646	13.63005	16.71520
	1.0	1.76214	4.40830	7.42029	10.45483	13.51736	16.60071
$b_0/a_0 = 2.0$							
0.05	0.8	1.84876	4.55571	7.62672	10.71887	13.81788	16.91419
	1.0	1.80859	4.52616	7.59265	10.66015	13.74357	16.83899
	1.0	[1.82577]	[4.54193]	[7.61742]	—	—	—
0.1	0.8	1.85423	4.57186	7.67258	10.78961	13.90756	17.02715
	1.0	1.82000	4.55155	7.64721	10.74665	13.85935	16.98048
	1.0	[1.83926]	[4.56738]	[7.67191]	—	—	—

Note: Data in parentheses were taken from Reference [18], and data in square brackets were taken from Reference [19]. The data in curly brackets were taken from Reference [31].

It is seen in Table 2 that the smaller the cross-sectional size factor  $b_0/a_0$  and aspect ratio  $\beta$  of the cylinder, the lower the natural frequencies of the cylinder–water interaction. However, the smaller the cylinder–water size factor  $\mu$ , the higher the natural frequencies of the cylinder–water interaction. To verify the accuracy of the proposed model, the first three non-dimensional frequency parameters of circular and elliptical cylinders completely submerged in water were compared with References Han and Xu [18] and Wang et al. [19]. The fundamental frequency of the circular cylinder completely submerged in water with  $\beta = 0.05$  was also compared with that from Li et al. [31] using the Timoshenko beam theory, as shown in Table 2. The first three natural frequencies from [18] and [19] and the fundamental frequency from [31] were converted into the corresponding non-dimensional frequency parameters  $\sqrt{\lambda_i}$  ( $i = 1, 2, 3$ ) given in Equation (29). It is seen that the present results are in good agreement with those from the three references. It should be noted that the present Bernoulli-Euler beam theory result of 1.74523 (corresponding to 2.0991 Hz)

is very close to the result of 1.74192 (corresponding to 2.0911 Hz) using the Timoshenko beam theory [31]. Compared with the fundamental frequency 1.77103 (corresponding to 2.1616 Hz) given by Han and Xu [18] using the Bernoulli-Euler beam model, the present result is in better accordance with that of Li et al. [31]. This shows that the Bernoulli-Euler beam theory does not bring significant computational errors for slender cylinders studied in the present analysis.

## 5. Conclusions

In this paper, a semi-analytical method was applied to investigate the characteristics of free vibration of a cylinder with a non-circular cross-section that was partially submerged in water. The analytical method was applied to obtain the solution of the velocity potential of the water, and the Galerkin method was applied to obtain the eigenfrequency equation of the cylinder–water interaction. Convergence studies and numerical results for elliptical cylinders partially submerged in water are given. The accuracy of NVAMI factor solutions was evaluated in detail, compared to the more accurate Galerkin solutions. Some interesting conclusions were obtained. It is shown that, for fundamental frequency, the NAVMI factor solutions can always give good estimations, especially for the cylinders entirely submerged in water. However, for the estimation of higher-order frequencies, the NAVMI factor approach can be used only when the cylinder–water density factor is very small, especially when the cylinders are partially submerged in water. The present semi-analytical method can serve as a benchmark test for numerical simulations of more complex computational fluid dynamics problems.

The Bernoulli-Euler beam theory was used because the present study focused on slender, solid, or hollow cylinders that were dominated by bending deformations. Thus, whether to use higher-order beam theories or shell theories does not bring significant computational errors. However, for short cylinders, more accurate results can be reached by adopting higher-order beam theories, such as the Timoshenko beam theory, rather than the Bernoulli-Euler beam theory because the transverse shear deformation tends to be more significant with larger  $\beta = a_0/H$ . For thin shell cylinders, more accurate results can be obtained by adopting shell theories if one wants to obtain the circumferential modes. It should be noted that the difference in the choice of theories does not affect the analytical process, especially for the analysis of the velocity potential of water.

The present study only gives the numerical results for a cantilever beam as an example; however, the entire analysis process is applicable for other boundary conditions.

Although the influence of the surface waves of water was neglected in the analysis, it should be noted that the present semi-analytical method is still applicable if the action of the surface waves needs to be considered. At this time, the solution of the velocity potential of water in Equation (10) should be obtained by adopting the Bessel functions instead of the modified Bessel functions.

**Author Contributions:** Conceptualization, H.H. and R.H.; methodology, H.H.; validation, H.H.; writing—original draft preparation, H.H. and Y.G.; writing—review and editing, H.H. and R.H. All authors have read and agreed to the published version of the manuscript.

**Funding:** This research was funded by the National Natural Science Foundation of China (52108149), the China Postdoctoral Science Foundation (2021M690623), and the Fundamental Research Program for the Jiangsu Provincial Colleges and Universities (21KJB560004).

**Institutional Review Board Statement:** Not applicable.

**Informed Consent Statement:** Not applicable.

**Data Availability Statement:** The data that support the findings of this study are available from the corresponding author upon reasonable request.

**Conflicts of Interest:** The authors declare no conflict of interest.

## References

1. Yun, G.J.; Liu, C.G. Nonlinear dynamic analysis of the deep-water bridge piers under combined earthquakes and wave actions. *Ocean Eng.* **2022**, *261*, 112076. [[CrossRef](#)]
2. Liu, H.B.; Chen, G.M.; Lyu, T.; Lin, H.; Zhu, B.R.; Huang, A. Wind-induced response of large offshore oil platform. *Petrol. Explor. Dev.* **2016**, *43*, 647–655. [[CrossRef](#)]
3. Liu, J.B.; Guo, A.X.; Li, H. Analytical solution for the linear wave diffraction by a uniform vertical cylinder with an arbitrary smooth cross-section. *Ocean Eng.* **2016**, *126*, 163–175. [[CrossRef](#)]
4. Xing, J.T.; Price, W.G.; Pomfret, M.J.; Yam, L.H. Natural vibration of a beam-water interaction system. *J. Sound Vib.* **1997**, *199*, 491–512. [[CrossRef](#)]
5. Zhu, Y.Y.; Wen, Z.Y.; Wu, J.R. The coupled vibration between column and water considering the effects of surface wave and compressibility of water. *Acta Mech. Sin.* **1989**, *6*, 657–667.
6. Cheung, Y.K.; Cao, Z.Y.; Wu, S.Y. Dynamic analysis of prismatic structures surrounded by an infinite fluid medium. *Earthq. Eng. Struct. Dyn.* **1985**, *13*, 351–360. [[CrossRef](#)]
7. Amabili, M. Effect of finite fluid depth on the hydroelastic vibrations of circular and annular plates. *J. Sound Vib.* **1996**, *193*, 909–925. [[CrossRef](#)]
8. Lin, H.Y.; Lee, J.N.; Sung, W.H. Vibration of an offshore structure having the form of a hollow column partially filled with multiple fluids and immersed in water. *J. Appl. Math.* **2012**, *2012*, 158983. [[CrossRef](#)]
9. Zhou, D.; Liu, W.Q. Hydroelastic vibrations of flexible rectangular tanks partially filled with liquid. *Int. J. Numer. Meth. Eng.* **2007**, *71*, 149–174. [[CrossRef](#)]
10. Zienkiewicz, O.C.; Bettess, P. Fluid-structure dynamic interaction and wave forces. An introduction to numerical treatment. *Int. J. Numer. Meth. Eng.* **1978**, *13*, 1–16. [[CrossRef](#)]
11. Kuhl, E.; Hulshoff, S.; Borst, R.D. An arbitrary Lagrangian Eulerian finite-element approach for fluid-structure interaction phenomena. *Int. J. Numer. Meth. Eng.* **2003**, *57*, 117–142. [[CrossRef](#)]
12. Jacobsen, L.S. Impulsive hydrodynamics of fluid inside a cylindrical tank and of fluid surrounding a cylindrical pier. *Bull. Seismol. Soc. Am.* **1949**, *39*, 189–204. [[CrossRef](#)]
13. Yang, X.J.; Li, Y.C.; Liu, Z.; Ou, Y.P. Experimental and numerical identification of wet frequencies for rectangular-section cantilever beam in water. *Open J. Acoust. Vib.* **2018**, *6*, 54–61. [[CrossRef](#)]
14. Wang, P.G.; Zhao, M.; Du, X.L. Simplified formula for earthquake-induced hydrodynamic pressure on round-ended and rectangular cylinders surrounded by water. *J. Eng. Mech.* **2019**, *145*, 04018137. [[CrossRef](#)]
15. Wei, K.; Bouaanani, N.; Yuan, W.C. Simplified methods for efficient seismic design and analysis of water-surrounded composite axisymmetric structures. *Ocean Eng.* **2015**, *104*, 617–638. [[CrossRef](#)]
16. Zhang, J.R.; Wei, K.; Qin, S.Q. An efficient numerical model for hydrodynamic added mass of immersed column with arbitrary cross-section. *Ocean Eng.* **2019**, *187*, 106192. [[CrossRef](#)]
17. Liu, Y.Y. HAMS: A frequency-domain preprocessor for wave-structure interactions—theory, development, and application. *J. Mar. Sci. Eng.* **2019**, *7*, 81. [[CrossRef](#)]
18. Han, R.P.S.; Xu, H.Z. A simple and accurate added mass model for hydrodynamic fluid-structure interaction analysis. *J. Frankl. Inst.-Eng. Appl. Math.* **1996**, *333*, 929–945. [[CrossRef](#)]
19. Wang, P.G.; Zhao, M.; Du, X.L. A simple added mass model for simulating elliptical cylinder vibrating in water under earthquake action. *Ocean Eng.* **2019**, *179*, 351–360. [[CrossRef](#)]
20. Yu, Y.; Ou, Y.P.; Liu, Z.; Li, Y.C. Simplified calculation method for dealing with added water mass for immersed cantilever cylinder. *Mech. Eng.* **2020**, *42*, 184–188. [[CrossRef](#)]
21. Deruntz, J.A.; Geers, T.L. Added mass computation by the boundary integral method. *Int. J. Numer. Meth. Eng.* **2010**, *12*, 531–550. [[CrossRef](#)]
22. Williams, A.N. Wave forces on an elliptic cylinder. *J. Waterw. Port Coast. Ocean Eng.* **1985**, *111*, 433–452. [[CrossRef](#)]
23. Li, Q.; Yang, W.L. An improved method of hydrodynamic pressure calculation for circular hollow piers in deep water under earthquake. *Ocean Eng.* **2013**, *72*, 241–256. [[CrossRef](#)]
24. Jiang, H.; Wang, B.X.; Bai, X.Y.; Zeng, C.; Zhang, H.D. Simplified expression of hydrodynamic pressure on deepwater cylindrical bridge piers during earthquakes. *J. Bridge Eng.* **2017**, *22*, 04017014. [[CrossRef](#)]
25. McCormick, M.E. Hydrodynamic coefficients of a monolithic circular offshore structure. *Earthq. Eng. Struct. Dyn.* **1989**, *18*, 199–216. [[CrossRef](#)]
26. Williams, A.N. Earthquake response of submerged circular cylinder. *Ocean Eng.* **1986**, *13*, 569–585. [[CrossRef](#)]
27. Yang, W.L.; Li, Q. A new added mass method for fluid-structure interaction analysis of deep-water bridge. *KSCE J. Civ. Eng.* **2013**, *17*, 1413–1424. [[CrossRef](#)]
28. Zhao, M.; Wang, L.X.; Huang, Y.M.; Wang, P.G.; Du, X.L.; Liu, J.B. A simplified added mass model for dynamic water pressure calculation of rectangle cylinder under earthquake. *J. Disaster Prev. Mitig. Eng.* **2020**, *40*, 174–180. [[CrossRef](#)]
29. Bhatta, D.D. Wave diffraction by circular and elliptical cylinders in finite depth water. *Int. J. Pure Appl. Math.* **2005**, *19*, 67–87.

30. Liang, K.M. *Mathematical Methods for Physics*, 5th ed.; Higher Education Press: Beijing, China, 2020; pp. 183–185.
31. Li, H.C.; Ke, L.L.; Yang, J.; Kitipornchai, S. Size-dependent free vibration of microbeams submerged in fluid. *Int. J. Struct. Stab. Dyn.* **2020**, *20*, 2050131. [[CrossRef](#)]

**Disclaimer/Publisher’s Note:** The statements, opinions and data contained in all publications are solely those of the individual author(s) and contributor(s) and not of MDPI and/or the editor(s). MDPI and/or the editor(s) disclaim responsibility for any injury to people or property resulting from any ideas, methods, instructions or products referred to in the content.